

Analysis of axial response of submarine pipeline to debris flow loading

Indranil Guha¹, Mark F. Randolph² and David J. White³

Technical Note submitted to Journal of Geotechnical and Geoenvironmental Engineering

Manuscript GTENG-9929: Revised 26th June 2020

¹ Indranil GUHA

Centre for Offshore Foundation Systems, University of Western Australia

35 Stirling Highway

Perth, WA 6009

Australia

Tel: +61 425 531 980

Email: guhanil@gmail.com

² Mark F. RANDOLPH (corresponding author)

Centre for Offshore Foundation Systems, University of Western Australia

35 Stirling Highway

Perth, WA 6009

Australia

Tel: +61 421 586 075

Email: mark.randolph@uwa.edu.au

³ David J White

Faculty of Engineering and Physical Sciences

University of Southampton

University Road

Southampton, SO17 1BJ

UK

Tel: +44 02380 596859

Email: david.white@soton.ac.uk

No. of words: 1975 (without abstract and references)

No. of tables: 2

No. of figures: 4

1 **Analysis of axial response of submarine pipeline to debris flow loading**

2 Indranil Guha, Mark F. Randolph and David J. White

3 **ABSTRACT**

4 This technical note presents simplified parametric solutions for the axial response of surface-
5 laid submarine pipelines subjected to axial drag from debris flows. In assessing the response of
6 pipelines impacted by debris flow emanating from a submarine landslide, both normal and axial
7 responses must be considered. Previous work has indicated that these can be decoupled, at least
8 as a first stage analysis. The most critical aspect of axial drag is the potential for the pipeline to
9 buckle. However, in order to make preliminary estimates of displacements and forces along the
10 pipeline prior to buckling, simple assumptions of elastic pipeline response with elastic perfectly
11 plastic interaction with the seabed are justified. These allow the development of parametric
12 solutions that contain only three non-dimensional quantities. The technical note documents the
13 solutions and illustrates their application for some typical input conditions.

14 **KEYWORDS**

15 Analysis, axial response, debris flow, submarine pipelines

16

17 INTRODUCTION

18 The offshore oil and gas industry commonly operates in deep water, beyond the continental
19 shelf, where infrastructure is vulnerable to a number of geohazards including submarine
20 landslides, mud and volcanoes, seismicity, shallow gas and gas hydrates (Kvalstad et al., 2001).
21 One of the most significant geohazards on the continental slope is the threat of submarine
22 landslides, which typically originate from the shelf-break but may run out several kilometres
23 into development zones or across pipeline routes. It is therefore necessary to consider both
24 normal and axial responses of pipelines impacted by debris flow, although the two modes of
25 response can be decoupled, at least as a first stage analysis (Randolph et al., 2010). Attention
26 here is focused on the axial response.

27 The most critical aspect of axial drag is the potential for the pipeline to buckle due to
28 compressive loading. However, in order to make preliminary estimates of displacements and
29 forces along the pipeline prior to buckling, it is sufficient to consider purely elastic response of
30 the pipeline, together with elastic perfectly plastic interaction with the seabed. The axial drag
31 resulting from the submarine slide may be considered as a uniform traction applied to the
32 pipeline over a defined zone.

33 These simple assumptions allow the development of parametric solutions to the problem that
34 contain only three non-dimensional quantities. The technical note documents the solutions and
35 illustrates their application for some typical input conditions. As an aside, it may also be noted
36 that many of the underlying relationships presented here may also be applied to related pipeline
37 problems, such as thermal expansion and contraction.

38 PROBLEM DEFINITION

39 The submarine slide-pipeline-seabed interaction problem may be divided into three parts: active
40 slide zone, passive plastic zone and elastic zone as shown in Figure 1. Within the slide zone,

41 the axial drag, F_{slide} , is assumed to overcome the ‘passive’ seabed resistance, resulting in a net
42 traction of F_{net} applied over the width of the submarine impact zone. Nominally this may be
43 considered as the difference between the slide loading and the passive seabed resistance,
44 although in practice the latter may be modified, and even eliminated, within the slide zone.
45 Beyond that zone, the seabed provides either an axial load-transfer stiffness (in the far-field
46 ‘elastic’ zone) or a limiting passive resistance $F_{passive}$ within the intermediate ‘passive’ zone.
47 Key axial tractions within each zone, and the loads and displacements at the interface points
48 between zones, are indicated in the schematic. The response in each zone is solved analytically
49 for the relevant boundary conditions in the following sections.

50 **Input parameters and dimensionless groups**

51 The perfectly straight pipe is defined by diameter, D , wall thickness, t submerged unit weight,
52 W' , and Young’s modulus, E , from which the axial rigidity EA can be calculated. The slide is
53 defined as a block zone of length, L_{slide} ; from symmetry of the problem, only the half slide
54 length, L_{AB} is considered here, with the axial force P_A in the pipeline at the centre of the slide
55 zone taken as zero. Any existing axial force distribution in the pipeline is ignored here, although
56 it would be relatively straightforward to extend the solutions presented to allow for that. The
57 length of the ‘passive plastic zone’ is L_{BC} , beyond which point (C onwards) the pipeline-seabed
58 interaction is elastic (Figure 1). The displacement at the centre of the slide, A , is u_A , at the
59 interface of ‘active’ and ‘passive’ zones, B , is u_B and at the interface between ‘passive’ and
60 ‘elastic’ zones, C is u_C . The axial load generated within the pipeline due to the slide movement
61 along the length is defined as P . The loads take values of P_A , P_B and P_C at the points
62 corresponding with u_A , u_B and u_C .

63 The axial load transfer stiffness between pipeline and seabed has been considered by Guha et
64 al. (2016). For a partially embedded pipeline **contacting the seabed over** chord width D'
65 (i.e. with $0 < D' \leq D$), the elastic load transfer stiffness may be approximated as

$$F / u = k_x = G_{D'} \quad (1)$$

66 where $G_{D'}$ is the seabed shear modulus at a depth of **the pipeline-seabed contact width** D' . More
67 detailed expressions, allowing for the pipeline embedment and exact profile of the seabed shear
68 modulus, are provided by Guha et al. (2016) and extend over a range of $\pm 20\%$ relative to the
69 above approximation. However, given the inevitable uncertainty in estimating shear modulus
70 values at very shallow depth, Equation (1) is considered sufficient.

71 The output quantities may be non-dimensionalised and expressed in terms of various input
72 properties. The maximum axial load, P_B , may be normalised by the axial elastic stiffness of the
73 pipe, EA , and presented as compressive strain, $\varepsilon = P/EA$; the axial displacement, u , may be
74 normalised by the slide length, L_{slide} , as u/L_{slide} . These normalised output parameters may then
75 be expressed in terms of normalised input parameters, i.e. the driving force, $a_1 = F_{net}L_{slide}/EA$;
76 passive resistance, $a_2 = F_{passive}L_{slide}/EA$; and pipe-soil stiffness, $a_3 = k_x L_{slide}^2/EA$. These three
77 groups can be shown to be sufficient to determine the longitudinal profile of load and
78 displacement of the pipe non-dimensionally.

79

80 Table 1 summarises the problem variables, together with relevant ranges for each that are
81 considered later. The range for the pile-soil axial stiffness k_x is quite large, reflecting conditions
82 from a small (0.1 m) diameter pipe half embedded in a soft clay with shear modulus of perhaps
83 500 kPa, to a large (1 m) diameter pipe shallowly embedded in dense sand with $G_{D'} \sim 10$ MPa.

84 From a practical point of view, very high combinations of the net force and length of slide
85 impact will lead to buckling of the pipeline, which is outside the scope of the solutions presented
86 here (see Guha, 2020), or at least localised plastic yield. Since the maximum normalised force
87 induced in the pipeline (i.e. average axial strain in the pipe) is, by inspection, $a_1/2$, an upper
88 limit of the normalised slide force is about 0.004 for elastic conditions to be maintained, and
89 rather less than that once buckling is considered.

90

91 **ANALYTICAL SOLUTION**92 **Elastic zone**

93 The axial load generated in the pipe due to the presence of frictional resistance of the seabed is

$$\frac{dP}{dx} = -F \quad (2)$$

94 The compressive strain, ε_x , of the pipeline (assumed elastic) is written in terms of the load, P ,
95 transmitted by the pipe at any length x ,

$$\varepsilon = -\frac{du}{dx} = \frac{-P}{EA} \quad (3)$$

96 Differentiating equation (3) and using equations (1) and (2) gives

$$\frac{d^2u}{dx^2} = \frac{F}{EA} = \frac{k_x}{EA} u \quad (4)$$

97 The solution of this equation is

$$u(x) = C_2 e^{\lambda x} + C_2 e^{-\lambda x} \quad (5)$$

98 where $\lambda = \sqrt{k_x / EA}$ is the inverse of a characteristic length with dimensions m^{-1} . To satisfy
99 the boundary conditions of zero displacement at large x , and $u = u_C$ at $x = x_C$, the displacement
100 variation within the elastic zone be expressed in terms of the displacement at the passive-plastic
101 and elastic zone interface by:

$$u(x) = u_C e^{-\lambda(x-x_C)} \quad (6)$$

102 The profile of load in the pipe may then be obtained by substituting equation (6) into equation
103 (3) and integrating to yield:

$$P = \frac{k_x}{\lambda} u_C e^{-\lambda(x-x_C)} \quad (7)$$

104 from which

$$P_C = \sqrt{k_x EA} u_C \quad (8)$$

105 In non-dimensional form, this may be written as

$$\frac{P_C}{EA} = \sqrt{\frac{k_x L_{slide}^2}{EA}} \frac{u_C}{L_{slide}} = \sqrt{a_3} \frac{u_C}{L_{slide}} \quad (9)$$

106 In principle, point C represents the interface between passive plastic and elastic zones (see
107 Figure 1), although if the active slide force is small the passive plastic zone may disappear. An
108 upper limit for the displacement at C is

$$u_{C-slip} = \frac{F_{passive}}{k_x} \quad \text{hence} \quad \frac{u_{C-slip}}{L_{slide}} = \frac{F_{passive} L_{slide}}{EA} \frac{EA}{k_x L_{slide}^2} = \frac{a_2}{a_3} \quad (10)$$

109 Substituting this into equation (9) gives the maximum load at the boundary of the elastic zone,
110 for the long pipe considered here, as

$$P_{C,max} = F_{passive} \sqrt{\frac{EA}{k_x}} \quad \text{hence} \quad \frac{P_{C,max}}{EA} = \frac{a_2}{\sqrt{a_3}} \quad (11)$$

111 **Passive plastic zone**

112 In general, there will be a passive plastic zone between the active slide zone and the elastic
113 zone, where slip occurs between the seabed and the pipe and the resistance force per unit length
114 is $F_{passive}$. The governing equations of the plastic zone are similar to those for the elastic zone,
115 but with $F = F_{passive}$ in equation (2). This results in a linear increase in force in the pipe between
116 points C and B , with

$$P_B = P_C + F_{passive} L_{BC} \quad \text{hence} \quad \frac{P_B}{EA} = \frac{P_C}{EA} + a_2 \frac{L_{BC}}{L_{slide}} \quad (12)$$

117 This may be used to determine the length of the passive zone, L_{BC} as

$$\frac{L_{BC}}{L_{slide}} = \frac{1}{a_2} \left(\frac{P_B}{EA} - \frac{P_C}{EA} \right) \quad (13)$$

118 When the passive zone $L_{BC} = 0$, point B coincides with point C leading to $P_B = P_C$. In general,

119 though, we may write $P_B \geq P_C$ and $L_{BC} \geq 0$.

120 Integration of equation (3), allowing for the linear variation of P between B and C , yields

$$\frac{u_B}{L_{slide}} - \frac{u_C}{L_{slide}} = \frac{(P_B + P_C)}{2EA} \frac{L_{BC}}{L_{slide}} = \frac{1}{2} \left[\left(\frac{P_B}{EA} \right)^2 - \left(\frac{P_C}{EA} \right)^2 \right] \frac{EA}{F_{passive} L_{slide}} = \frac{1}{2a_2} \left[\left(\frac{P_B}{EA} \right)^2 - \left(\frac{P_C}{EA} \right)^2 \right] \quad (14)$$

121 For a small active slide load (or strong passive resistance), u_C may not reach the elastic limit of

122 u_{C-slip} , in which case $L_{BC} = 0$, $P_B = P_C$ and $u_B = u_C$.

123 Active zone

124 In the active zone the interaction between the pipe and the soil is assumed to be plastic. The

125 displacement is taken as u_A at the centre of the slide ($x = 0$) from symmetry. Similarly, the axial

126 force P_A in the pipe is zero at $x = 0$, and increases linearly to P_B at the edge of the slide material,

127 where

$$P_B = \frac{F_{net} L_{slide}}{2} \quad \text{hence} \quad \frac{P_B}{EA} = \frac{F_{net} L_{slide}}{2EA} = \frac{a_2}{2} \quad (15)$$

128 Note that P_B represents the largest axial force generated in the pipeline, and hence the maximum

129 compressive strain in the pipe is $\epsilon_{max} = a_1/2$.

130 Integrating equation (3), for the linear variation of P from zero at A to $a_1/2$ at B , yields

$$u_A - u_B = \frac{P_B L_{slide}}{4EA} = \frac{F_{net} L_{slide}^2}{8EA} \quad \text{hence} \quad \frac{u_A}{L_{slide}} = \frac{u_B}{L_{slide}} + \frac{a_1}{8} \quad (16)$$

131 Summary of solution

132 For convenience the main expressions are summarized here in non-dimensional form. The key
133 loads may be expressed as

$$\frac{P_A}{EA} = 0; \frac{P_B}{EA} = \frac{a_1}{2}; \frac{P_C}{EA} = \text{Min} \left(\frac{a_1}{2}, \frac{a_2}{\sqrt{a_3}} \right) \quad (17)$$

134 The length of the (plastic) passive zone is given by

$$\frac{L_{BC}}{L_{slide}} = \text{Max} \left(0, \frac{a_1}{2a_2} - \frac{1}{\sqrt{a_3}} \right) \quad (18)$$

135 The displacements at key points are

$$\begin{aligned} \frac{u_A}{L_{slide}} &= \frac{a_1}{8} + \text{Max} \left(\frac{a_1}{2\sqrt{a_3}}, \frac{1}{8} \frac{a_1^2}{a_2} + \frac{1}{2} \frac{a_2}{a_3} \right) \\ \frac{u_B}{L_{slide}} &= \text{Max} \left(\frac{a_1}{2\sqrt{a_3}}, \frac{1}{8} \frac{a_1^2}{a_2} + \frac{1}{2} \frac{a_2}{a_3} \right) \\ \frac{u_C}{L_{slide}} &= \text{Min} \left(\frac{1}{2} \frac{a_1}{\sqrt{a_3}}, \frac{a_2}{a_3} \right) \end{aligned} \quad (19)$$

136 These relationships are illustrated in Figure 2, which shows the length of the plastic zone L_{BC}
137 as a function of the normalised net slide force $a_1 = F_{net}L_{slide}/EA$, and Figure 3, which shows
138 corresponding key displacement ratios. As might be expected intuitively, the length of the
139 plastic zone grows proportionally with the ratio of driving to resisting force ($F_{net}/F_{passive}$), with
140 almost no influence of the elastic stiffness ratio $a_3 = k_x L_{slide}^2/EA$ apart from at very low ratios
141 of $F_{net}/F_{passive}$.

142 In a similar vein, the magnitude of displacements u_A and u_B , both normalised by L_{slide} , grow
143 proportionally with the ratio of driving to resisting force, except where that ratio falls below
144 unity. Once $F_{net}/F_{passive}$ reduces below unity, the maximum displacement at the mid-point of the
145 slide (u_A) asymptotes to a plateau that corresponds to the pipe compression within the slide
146 zone, essentially half the ratio $0.5a_2/a_3$, as the displacement at B reduces towards zero. In most
147 cases the displacement at interface between passive and elastic zones (u_C) is negligible.

148 **EXAMPLE NUMERICAL SOLUTION**

149 As a check on the analytical solution, and to explore the effect of different slide loading on a
150 given pipeline, three example cases are considered here, with results compared with those
151 obtained from finite element analysis (Guha, 2020). The three cases were for a 1 m diameter
152 pipeline with D/t of 25, subjected to slide loading of 11.9 kN/m over slide lengths of 100, 300
153 and 500 m, beyond the seabed passive resistance is 3.8 kN/m. The input data and corresponding
154 normalised parameters are summarised in Table 2.

155 Figure 4 shows the resulting profiles of (a) axial force, and (b) axial displacement along the
156 pipeline for the three cases. Note the axial displacements have been factored up by 1000.
157 Corresponding displacements from finite element analyses (Guha, 2020) are shown for
158 comparison. The zones of slide loading, plastic passive resistance and elastic resistance are
159 colour coded, respectively blue, red and green. The finite element data confirm the accuracy of
160 the analytical solution. Overall, the results also show that, provided the pipe does not fail
161 through plasticity or buckling, the axial displacements remain rather small, varying
162 quadratically with the magnitude of total slide load ($F_{net}L_{slide}$) and, for these cases, ranging
163 between 2.7 mm and 62 mm.

164 CONCLUDING REMARKS

165 This technical note has documented a simple analytical solution to the distribution of axial
166 force, strain and displacements in a pipeline loaded axially by a debris flow. The solutions
167 facilitate simple calculation of the potential for failure of a pipe due to plastic strains or (in a
168 broader context not considered here) by lateral buckling.

169 DATA AVAILABILITY STATEMENT

170 All data, models, and code generated or used during the study appear in the submitted article.

171 ACKNOWLEDGEMENTS

172 This work forms part of the activities of the Centre for Offshore Foundation Systems (COFS),
173 established in 1997 under the Australian Research Council's Special Research Centres Program,
174 and supported (2010-2017) as a node of the Australian Research Council's Centre of Excellence
175 for Geotechnical Science and Engineering, and through the Fugro Chair in Geotechnics, the
176 Lloyd's Register Foundation Chair and Centre of Excellence in Offshore Foundations and the
177 Shell Chair in Offshore Engineering.

178 REFERENCES

- 179 Guha, I. (2020). *Structural Analysis of Submarine Pipelines Under Submarine Slide and*
180 *Thermal Loading*. Forthcoming PhD thesis, The University of Western Australia.
- 181 Guha, I., Randolph, M.F. and White, D.J. (2016). Evaluation of elastic stiffness parameters for
182 pipeline-soil interaction. *J. of Geotechnical and Geoenvironmental Engineering*, ASCE,
183 04016009-(1-12).
- 184 Kvalstad, T.J., Nadim, F., and Harbitz, C.B. (2001). Deepwater geohazards: geotechnical
185 concerns and solutions. *Proc. Offshore Technology Conference*, Houston, Paper OTC 12958.

186 Randolph, M.F., Seo, D., and White, D.J. (2010). Parametric solution of slide impact on
187 pipelines. *J. of Geotechnical and Geoenvironmental Engineering*, 136(7), 940-949.

188

189 Table 1: Summary of range of input and output parameters

Input parameters	Range	Units
Pipeline diameter, D	0.1 - 1	m
Pipeline diameter to wall thickness ratio, D/t	13 - 20	
Elastic modulus of pipeline, E	210	GPa
Length of slide loading on pipeline, L_{slide}	50 – 1000	m
Net slide force on pipeline, F_{net}	0.1 – 10	kN/m
Passive seabed frictional resistance force, $F_{passive}$	0.02 – 10	kN/m
Pipe-soil elastic axial stiffness, k_x	50 – 10,000	kPa
Adopted range of non-dimensional input parameters		
Normalised slide loading, a_1	$F_{net} \cdot L_{slide} / EA$	0.000001 – 0.01
Normalised passive resistance, a_2	$F_{passive} \cdot L_{slide} / EA$	0.000001 – 0.01
Normalised pipe-soil elastic stiffness, a_3	$k_x \cdot L_{slide}^2 / EA$	0.01 - 10000
Non-dimensional output quantities		
Axial loads	$P_B / EA, P_C / EA$	
Length of passive zone	L_{BC} / L_{slide}	
Displacements	$u_A / L_{slide}, u_B / L_{slide}, u_C / L_{slide}$	

190

191

192 Table 2: Input parameters for numerical examples

Input parameters	Case 1	Case 2	Case 2
Pipeline diameter, D (m)	1	1	1
Diameter to wall thickness ratio, D/t	25	25	25
Cross-sectional stiffness, EA (MN)	25300	25300	25300
Length of slide, L_{slide} (m)	100	300	500
Net slide loading, F_{net} (kN/m)	11.9	11.9	11.9
Passive resistance, $F_{passive}$ (kN/m)	3.8	3.8	3.8
Pipe-soil elastic axial stiffness, k_x (kPa)	6400	7000	8000
Normalised slide loading, a_1	0.000047	0.000141	0.000236
Normalised passive resistance, a_2	0.000015	0.000045	0.000074
Normalised pipe-soil elastic stiffness, a_3	2.5	24.9	78.9

193

194

195

196

197

198 **Figure Captions**

199 Figure 1 Idealisation of axial slide pipeline interaction

200 Figure 2 Length of passive zone, L_{BC}

201 Figure 3 Normalised axial displacements of pipe

202 Figure 4 Results of three example cases

203

204

205

206

207

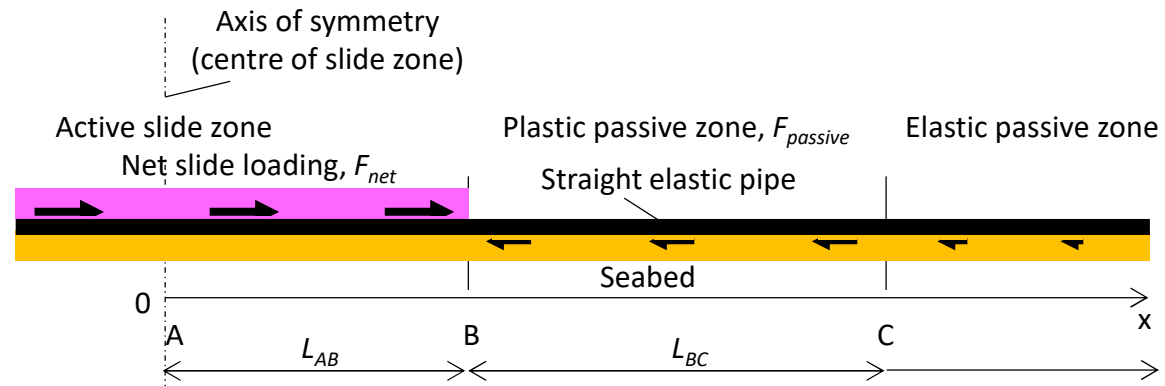
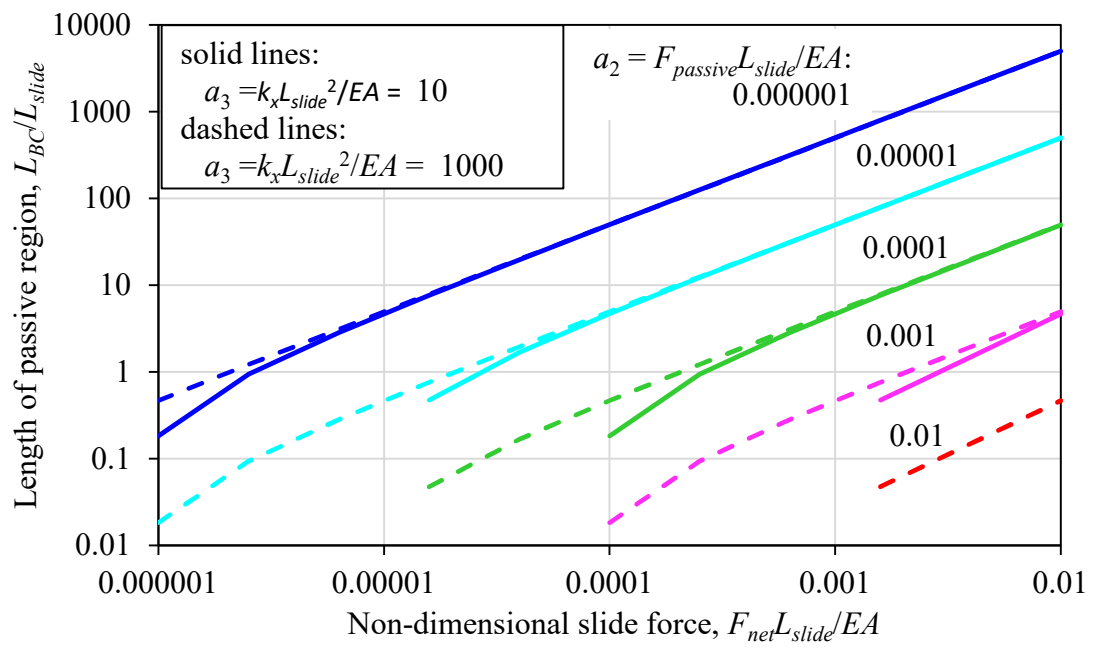


Figure 1 Idealisation of axial slide pipeline interaction

Figure 2 Length of passive zone, L_{BC}

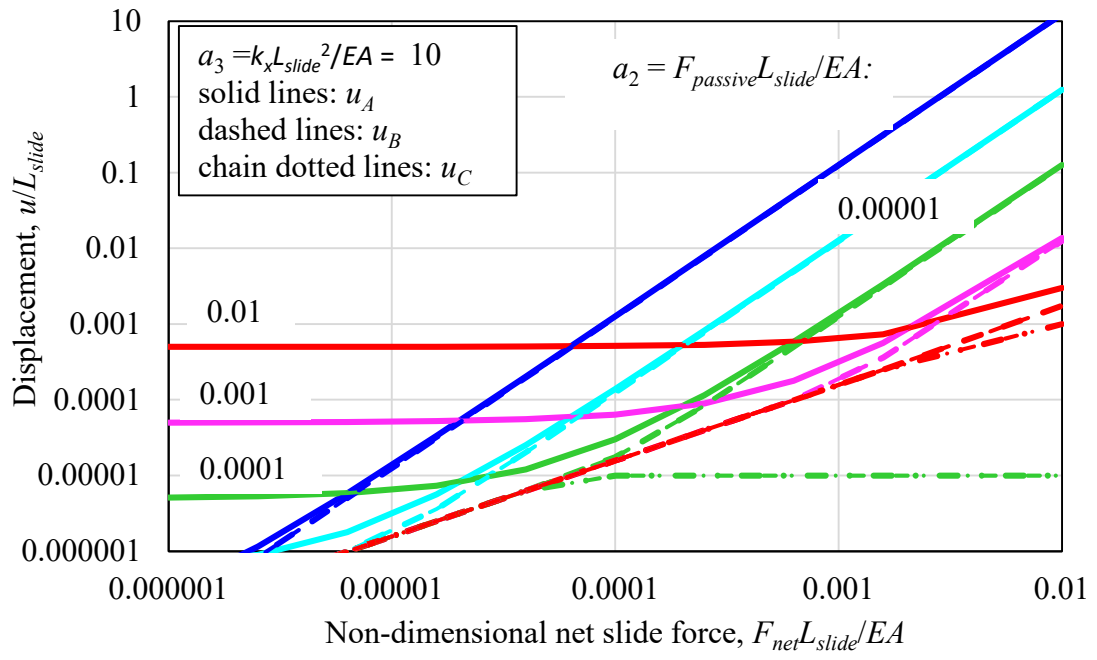
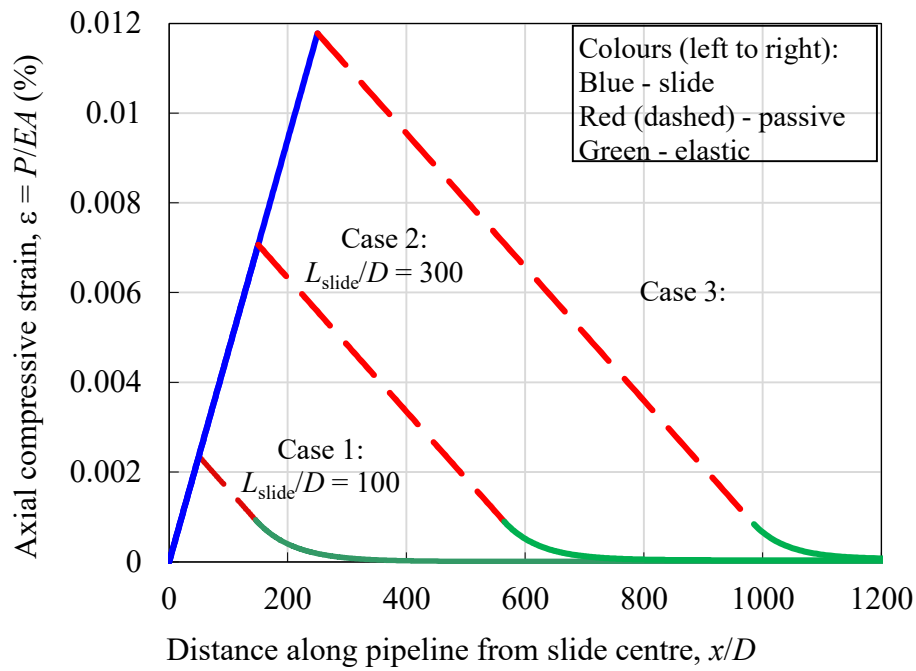
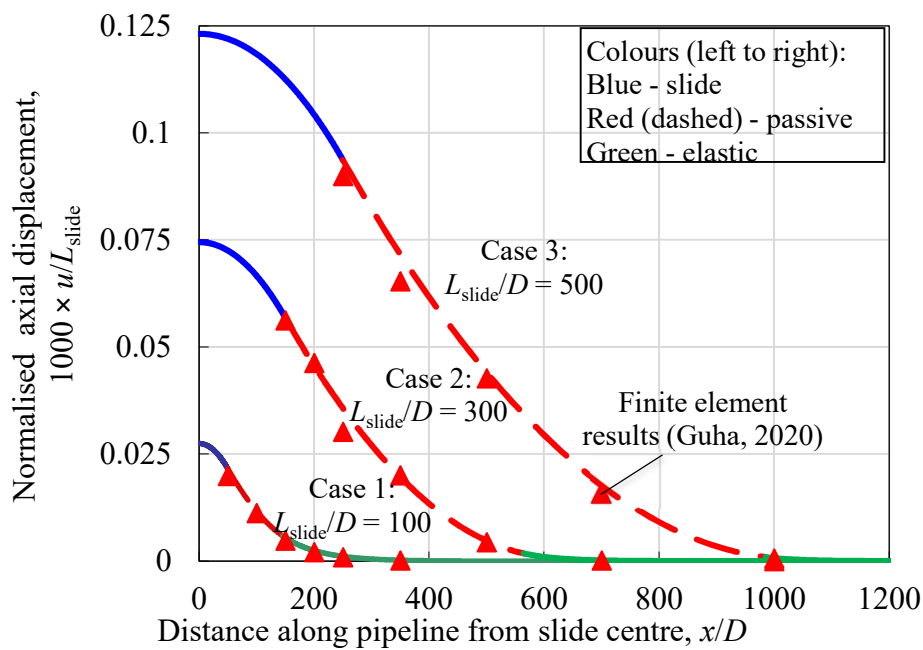


Figure 3 Normalised axial displacements of pipe



(a) Distribution of axial strain along the pipeline



(b) Distribution of axial displacements along the pipeline

Figure 4 Results of three example cases